Dear Thomas,

Thank you very much for your effort reading our manuscript so carefully and for your valuable advices. We strongly believe that the suggested changes and additions improved the manuscript a lot. Please find below a point-by-point reply to all your recommendations (in blue).

1) For me it is not perfectly clear if the merit function defined here (MNR) is really the most important point. Usually the distance information is en-coded in the first part of the time trace and the longer times are only necessary to fit well the intermolecular background function – a necessary procedure to obtain reliable distance information. The question is how large the increasing noise at the end of the time trace is important for this purpose. This point should be discussed and clarified.

We have added an additional chapter in the SI where we discuss the MNR as a function of merit and up to which point of the DEER trace it has to been taken into account.

S2 The MNR as the function of merit

Here, we want to discuss whether the MNR is a suitable function of merit for the determination of distance distributions and up to which time point in the DEER trace, the MNR needs to be evaluated to serve this purpose. Therefore, we performed simulations with a model distance distribution p_0 that is based on the narrow distance distribution of the model system used in this study. We approximated the experimentally obtained distance distribution with a Gaussian with a mean at 5.08 nm and a standard deviation of 0.08 nm. We varied the background density in ten steps from k = 0.01 1/µs to k = 0.3 1/µs in combination with a low, medium and high noise level (noise σ_0 = 0.02, 0.05 and 0.1) that was added to the DEER trace. The background dimension was set to d = 3 and a modulation depth of 0.5 was used. The DEER traces were simulated in the time domain up to 8 µs. For each parameter set we generated ten different traces. To compare the background correction by division (Jeschke et al., 2006) with the kernel inclusion approach as described in (Fábregas Ibáñez and Jeschke, 2020) we analysed all simulated DEER traces with both methods. We did not fit the background but used the true background function. The regularisation parameter was chosen according to the generalised cross-validation method. The quality of the resulting distance distributions p was estimated by the Euclidian distance D from the true distance p_0:

$$D(p, p_0) = \|p - p_0\|_2 \quad (1)$$

The MNR of the form factor F was calculated as described in the main text up to a limit of 7 µs according to equation (13) of the main text.

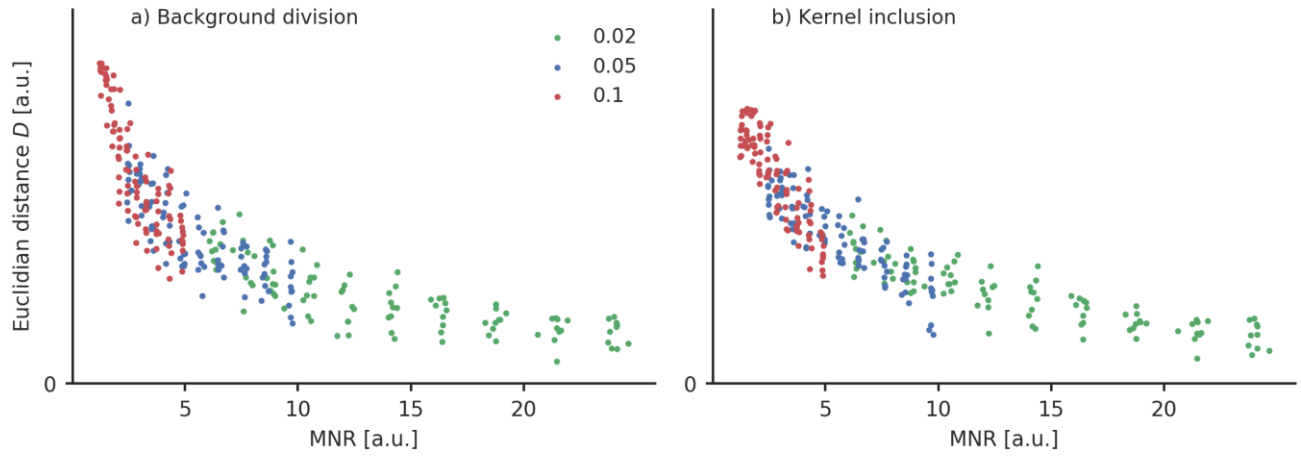

Figure S2: The Euclidian distance D of the real and calculated distance distribution as defined in equation (1) is plotted as a function of the MNR. Each dot represents a simulated DEER trace with either low (σ_0 = 0.02, green), medium (σ_0 = 0.05, blue) and high (σ_0 = 0.1, red) noise. The background correction was performed by (a) dividing the DEER trace by the background and (b) including the background in the kernel.

In Fig. S2, the quality of the determined distance distribution was plotted as a function of the determined MNR for both a background correction by division (Fig. S2a) and a kernel inclusion approach (Fig. S2b). For each noise level the MNR only depends on the density of the background as all other parameters are kept constant and only the background density is varied. So a lower MNR corresponds to a higher background density rate and vice versa. For the low noise level (σ_0 = 0.02), the quality of the determined distance distributions only varies a little for different background density rates. For medium (σ_0 = 0.05) and high (σ_0 = 0.1) noise levels, however, the dependency of the quality of the determined distance distribution decreases significantly with a decreasing MNR. If the MNR is only evaluated up to an early point of the form factor, the information of the background decay rate is lost in this case and is not properly included in the MNR as the MNR would then depend nearly exclusively on the given noise level.

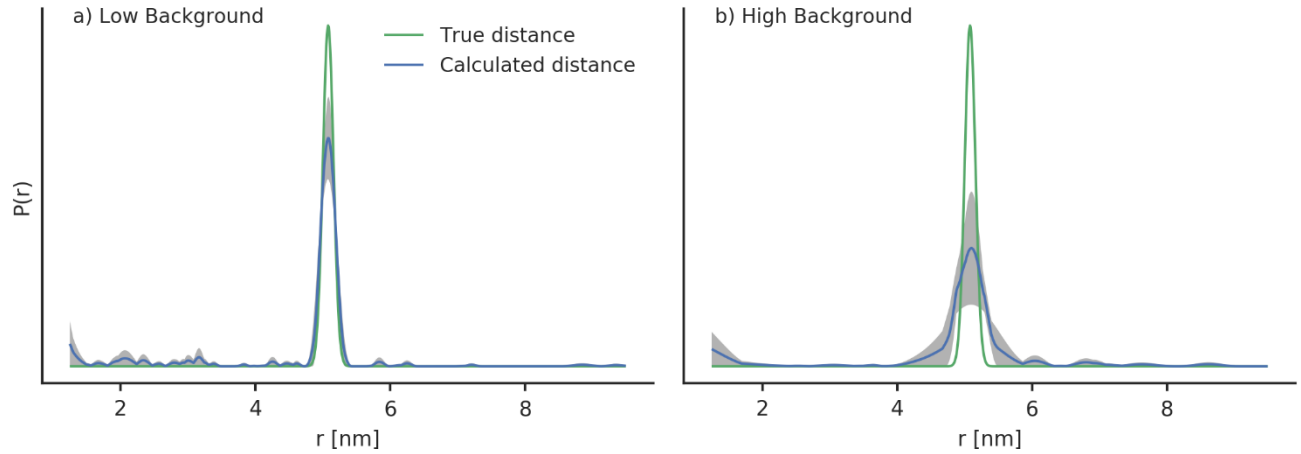

Figure S3: An exemplary distance distribution obtained for a medium noise level (σ_0 = 0.02) with (a) a low background density (k = 0.01 MHz) and (b) a high background density (k = 0.3 MHz). The grey area shows the area that is covered by the

calculated distance distribution for ten exemplary DEER traces. The mean of the shaded area is drawn in blue and the true distance is drawn in green.

A closer inspection reveals that whereas the obtained distance distributions for high background densities reproduce the mean of the distance distribution correctly, they overestimate the width of the distribution and the distance appears to be broader as it is (see Fig. S3 for an exemplary data set). Depending on the information that shall be obtained by the DEER measurements, the mean of the distance distribution might suffice. However, if high resolution distance distributions shall be obtained, it seems to be important to optimise the MNR up to the limit which is given by equation (13) of the main text. The comparison of both background correction methods shows that the kernel inclusion gives better results particularly for a high noise and a high background decay. It should therefore be considered as the superior method. However, the correlation between the quality of the determined distance distribution and the MNR is still valid. This is why, we consider the MNR as a proper function of merit, even if the kernel inclusion approach is used.

For a more comprehensive study, the effect of the MNR on the quality of the obtained distance distribution could also be tested for distance distributions with different distance ranges and widths. Such a detailed study was, however, beyond the scope of the this manuscript.

2) The manuscript talks about the intermolecular background function but for the larger spin concentration, where most of the experiments are performed and most of the conclusions are taken from, the original time traces including this background function are not shown! This has to be included! It is not enough to show the background density k as in Figure S11.

We have added a new figure S17 with full DEER traces and background functions of both samples for rectangular and Gaussian pulses.

S20 Background decay of the DEER traces

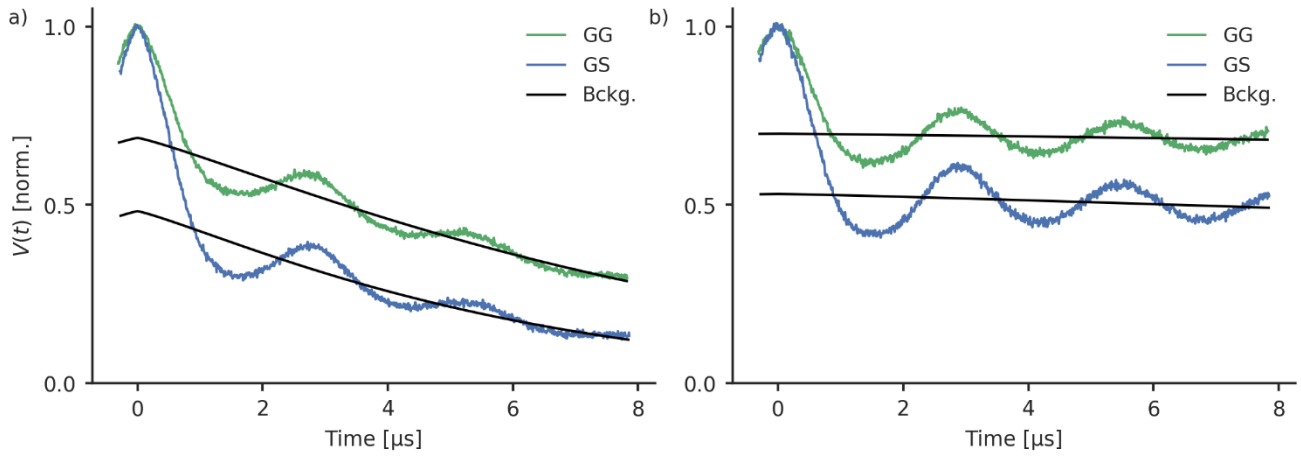

Figure S17: The (normalised) experimental raw data of the sample with a 80 µM (a) and 30 µM (b) ligand concentration. The settings for GG (green) were performed with a 100 %pulse amplitude and a 70 MHz offset. For GS (blue), the observer pulses were at a frequency of 70 MHz offset from the centre of the resonator. The pump pulses were HS{1,1} pulses, with the parameters $\beta = 8/t_p$, $t_p = 100$ ns, $\Delta f = 110$ MHz and an offset from the observer pulse of 90 MHz. Note that the acquisition time for the sample with lower concentration was longer in order to reach a similar noise level for both cases. The corresponding form factors are depicted in Fig. S11.

3) In Figure S10 an unexpected large suppression of the echo intensity by longer broadband pump pulses is shown. This is totally unexpected for the given bandwidth of these pulses and contrary to own experiences, where longer pulses show better frequency shapes! If the pulses are generated by the Bruker soft-ware some care has to be taken to use the right amplitude setting, especially the frequency runs over the carrier frequency (from minus offsets to plus offsets). The pulse profiles shown in Figure S7 are probably only calculated pulses and not really measured ones? Experimentally recording them including the resonator profile (which also seems somewhat suspicious to me) might give some hints on what is going on here! This issue is rather important for the conclusions drawn here from the shaped pulses!

We thank Thomas Prisner for this hint. We have redone the experiments and added measured inversion profiles of the pulses. We also want to note that the frequency of the calculated pump pulses does not run over the carrier frequency of the spectrometer because the pulse offset to the observer frequency (carrier frequency) is included. The resonator profile looks unusual (increase at the lower frequency end) because the used resonator is a dual mode resonator. In the figure below the resonator profile recorded over a larger range can be seen. Note that this was recorded with Gd and a different microwave power, hence the different values for the nutation frequency.

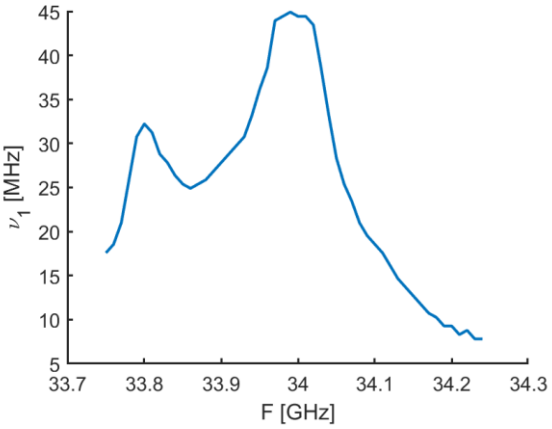

However, it was not feasible to use the second mode for the DEER measurements because of the limited width of the nitroxide EDFS spectrum. In order to discuss the issue with the 200 ns and 400 ns pump pulses, we have replaced S12 and S13 with the following new chapter, where we have also included measured inversion profiles of the broadband shaped pump pulses.

S13 The influence of the length of broadband shaped pump pulses

Tests with broadband shaped pump pulses with pulse lengths of 200 ns and 400 ns showed that they do not lead to an overall performance increase. This is shown here exemplary by comparing the performance of HS{1,1} pump pulses and Gaussian observer pulses (Fig. S12). There are indeed some pump pulses (for example a HS{1,1} pulse with $\beta = 10/t_p$ and $\Delta f =$ 110 MHz) that show an improvement with a longer pulse length, however there is no overall gain by using a pump pulse length of 200 ns.

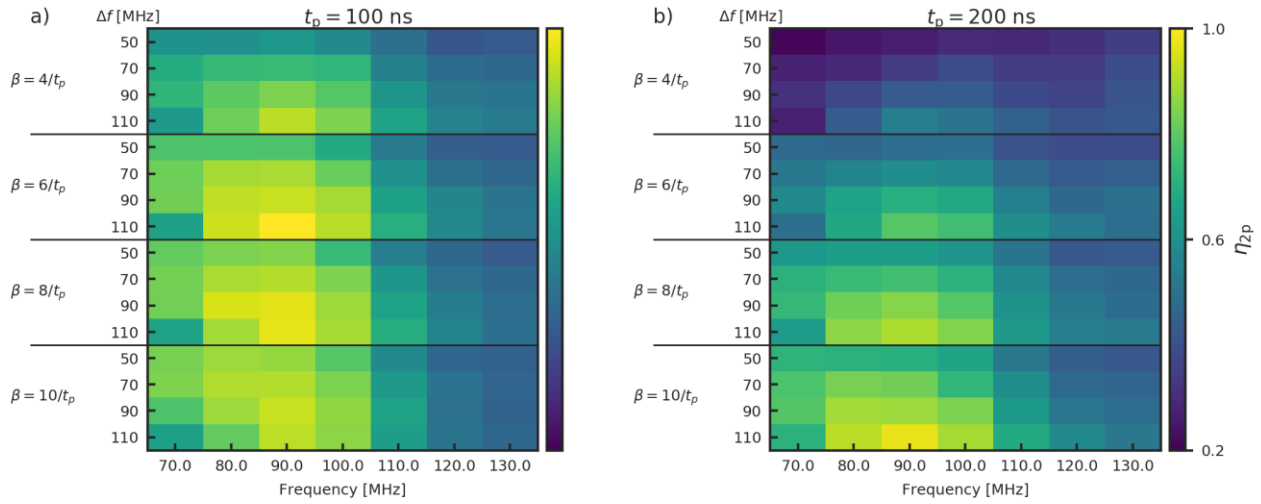

Figure S12: HS{1,1} pump pulses of (a) 100 ns and (b) 200 ns length. The observer pulses were Gaussian pulses with 100 % intensity at an observer position with a 90 MHz offset from the centre of the resonator profile and a pulse length of 56 ns for the π pulse. The colour bars are normalised to the same value so that both heat maps are comparable.

We noticed that a major problem with longer broadband shaped pump pulses is that the intensity of the echo can be reduced (Fig. S13a). For a pump pulse offset of 90 MHz, the echo intensity at the zero time of the DEER trace is reduced significantly when increasing the pump pulse lengths from 100 ns over 200 ns to 400 ns.

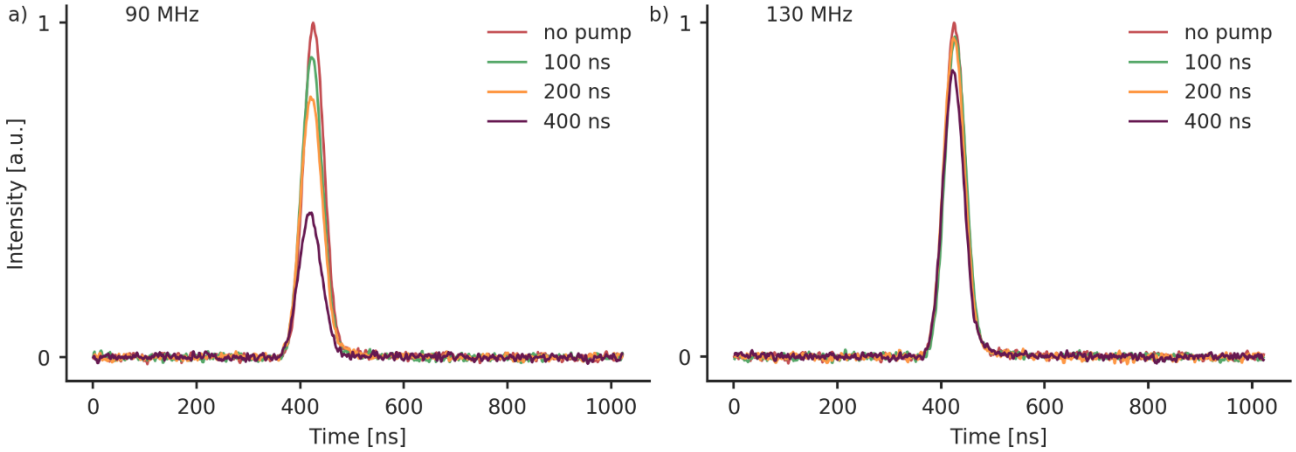

Figure S13: The echo at the zero time of the DEER trace. The observer pulses were Gaussian pulses with 100 % intensity at an observer position with a 70 MHz offset from the centre of the resonator profile and a pulse length of 56 ns for the π pulse. The pump pulses were HS{1,1} pulses with $\beta = 8/t_p$ and $\Delta f = 110$ MHz. The offset between the pulses is (a) 90 MHz and (b) 130 MHz.

A comparison of the calculated inversion profiles of the respective pulses (Fig. S14a-c) shows that, whereas the 100 ns pulse should lead to an incomplete inversion, a nearly complete inversion can be expected for the longer pulses. Furthermore, the longer pulses should have slightly steeper excitation flanks. Those trends can indeed be found for the measured inversion profiles. There are some deviations of the measured and calculated inversion profiles. The measured inversion profile of the 100 ns pulse shows an increased frequency width compared to the calculated profile. Furthermore, there is bump in the centre

of the frequency sweep. The measured inversion profiles of the longer pulses show the expected steep frequency flanks that can also be seen in the simulation. The inversion profiles of the 200 ns and the 400 ns pulses show a small asymmetry around the centre of the frequency sweep. We assign these deviations to instrumental pulse distortions caused by the spectrometer.

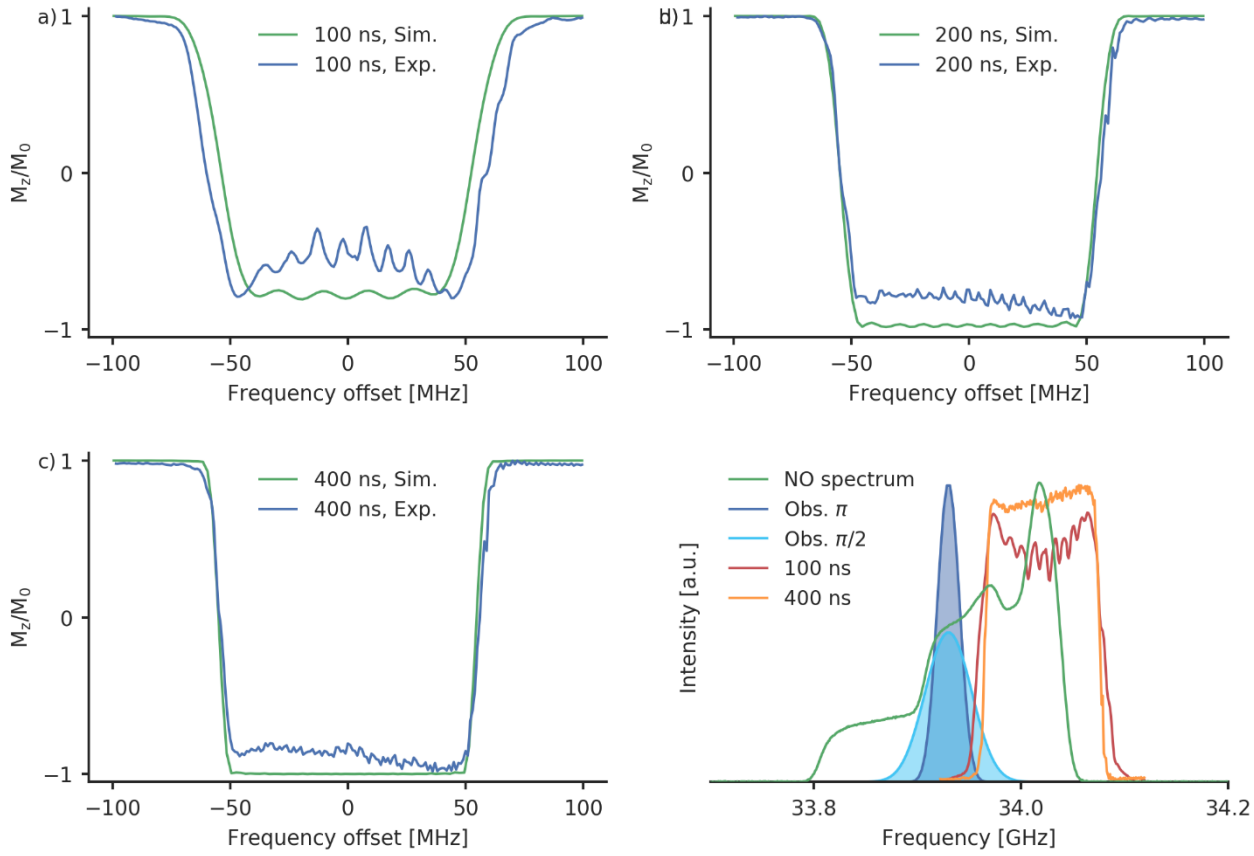

Figure S14: Calculated and measured inversion profiles of a HS{1,1} pulse with $\beta = 8/t_p$ and $\Delta f = 110$ MHz and a pulse length of (a) 100 ns, (b) 200 ns and (c) 400 ns. A 400 ns calculated pump excitation profiles next to the observer pulse excitation profiles is shown in (d).

It is expected that steeper excitation flanks lead to a smaller overlap with the observer pulses and therefore a smaller effect on the echo intensity. Despite this is the case here as well (Fig. 14d), the overlap is not reduced completely and 400 ns pulse still has some remaining spectral overlap with the observer pulses. We assume that the contradictive findings concerning the echo intensity here are caused by this remaining small overlap. It could become more perturbing for longer pulses as the overall energy of the pulses increases with the pulse length and therefore potential disturbances might be enhanced. A measurement with an larger offset between the pulses at 130 MHz shows that the echo decrease is indeed reduced (Fig. S13b) when the overlap gets smaller. Despite leading to a higher echo intensity, such a high offset is not favourable for nitroxode-nitroxide DEER, because of the limited width of the nitroxide spectrum.

4) The concentration dependence of the behavior is only discussed in a rather trivial and non-quantitative manner, despite the fact that it showed to be the major parameter influencing the improvement by the broadband pulses (comparison Figure6 and 7). That lower concentrations of spins are advantageous, especially for larger distances or broader distance distributions is well known in the community. Because broadband pulses might be especially interesting for these kind of systems, this should be discussed more quantitatively! The discussion in the SI including Figure S13 and the text after it is only very qualitative and rather trivial.

We have replaced the discussion in the SI with this section

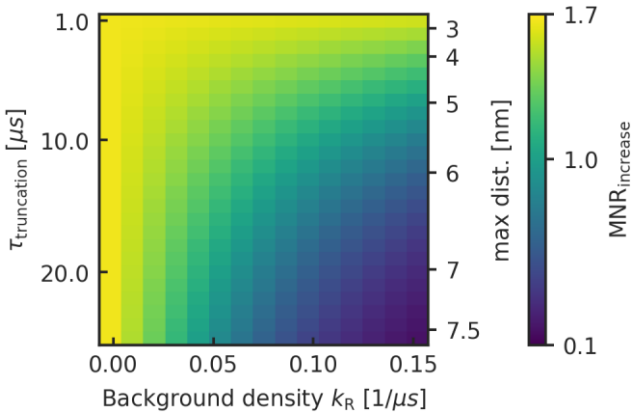

Figure S18: The MNR-ratio of adiabatic and rectangular pulses as a function of the background density (with rectangular pulses) and the $\tau_{truncation}$-time. The corresponding maximum distance according to equation (13) of the main text is also depicted. As the background density reflects the concentration the x-axis is a measure for the concentration of the spin centres. In our sample with 80 µM, we had a background density k_R of 0.1 with rectangular pulses.

Figure S18 shows that the performance of shaped pulses can heavily depend on the circumstances of the measurement. For a maximum distance below 4 nm ($\tau_{truncation} \approx 5$ µs), a MNR increase can be expected for all realistic concentration ranges. This is not the case if a longer distance shall be detected. For maximum distances around 5 nm, the MNR increase goes to 1 for high background densities of $k_R = 0.15$ 1/µs, which corresponds to very high concentrations > 100 µM. Typical concentrations for DEER measurements are around 50 µM, which here corresponds to a $k_R \approx 0.06$ 1/µs. For this concentration, a significant increase in the MNR can only be expected up to a truncation time of $\tau_{truncation} = 10$ µs, which is equal to a maximum distance of approximately 6 nm.

As broadband shaped pulses are particularly interesting for long distances, the calculations were performed up to a rather long truncation time of 25 µs (maximum distance of approximately 7.5 nm). For distances in the range > 6 nm, only with concentrations in the range of 10-30 µM ($k_R \approx 0.01$-0.04 1/µs) a significant increase in the MNR due to broadband shaped pump pulses can be expected. The MNR increase drops quickly when higher concentrations are used. For a maximum distance of 7.5 nm and for concentrations over approximately 40 µM no increase can be expected any more due to broadband shaped pulses. If a concentration of 80 µM is used, the MNR is about to decrease to roughly 40 % when switching to broadband

shaped pulses. It is known that diluting the sample is favourable if long distances shall be detected because it increases the phase memory time of the echo (Schmidt et al., 2016). When broadband shaped pump pulses, the higher background decay adds an additional point for carefully choosing the concentration of the sample and it seems to be advisable to avoid high concentrations.

5) Minor point: In the supporting information equation (2) is wrong. After that there is a spelling error (ration).

We thank Thomas Prisner for this remark. We have corrected the spelling mistakes.